Journal of Diabetes Science and Technology
Volume 7, Issue 5, September 2013
© Diabetes Technology Society

ORIGINAL ARTICLE

Signal Processing Algorithms Implementing the "Smart Sensor" Concept to Improve Continuous Glucose Monitoring in Diabetes

Andrea Facchinetti, Ph.D., Giovanni Sparacino, Ph.D., and Claudio Cobelli, Ph.D.,
on behalf of the AP@home Consortium

Abstract

Glucose readings provided by current continuous glucose monitoring (CGM) devices still suffer from accuracy and precision issues. In April 2013, we proposed a new conceptual architecture to deal with these problems and render CGM sensors algorithmically smarter, which consists of three modules for denoising, enhancement, and prediction placed in cascade to a commercial CGM sensor. The architecture was assessed on a data set consisting of 24 type 1 diabetes patients collected in four clinical centers of the AP@home Consortium (a European project of 7th Framework Programme funded by the European Committee). This article, as a companion to our prior publication, illustrates the technical details of the algorithms and of the implementation issues.

J Diabetes Sci Technol 2013;7(5):1308–1318

Introduction

Subcutaneous continuous glucose monitoring (CGM) sensors are minimally invasive portable devices able to measure (and visualize in real time) glycemia in the interstitium almost continuously (1–5 min sampling period) for approximately seven consecutive days.[1–5] The nature of CGM data opened the doors to the realization of investigations and applications that were hindered by the sparseness of self-monitoring of blood glucose (SMBG) measurements.[6] For instance, CGM data can be analyzed retrospectively to evaluate glucose variability[7] and used in real time to generate alerts when glucose approaches, or exceeds, hypoglycemic or hyperglycemic thresholds[8] (see, for instance, referenced work for a quantification of potential reduction of number and duration of hypoglycemic events performed in an *in silico* environment[9,10] and their preliminary application in clinical research centers[11–13]). Moreover, CGM sensors are a key element of artificial pancreas (AP) research prototypes, i.e., minimally invasive systems for subcutaneous insulin infusion driven by a closed-loop control algorithm.[14–20]

However, the performance of modern CGM sensors is still considered inferior to that of SMBG measurements and laboratory systems.[21–23] This is critical both for daily life therapy, because CGM sensors are not approved to be used in place of SMBG for therapy adjustment, and in research clinical trials, because the suboptimal performance of CGM

Author Affiliation: Department of Information Engineering, University of Padova, Padova, Italy

Abbreviations: (AP) artificial pancreas, (BG) blood glucose, (CGM) continuous glucose monitoring, (ESOD) energy of second-order differences, (MARD) mean absolute relative difference, (PH) prediction horizon, (SMBG) self-monitoring of blood glucose, (T1DM) type 1 diabetes mellitus

Keywords: continuous glucose monitoring, denoising, filtering, prediction, sensor calibration

Corresponding Author: Claudio Cobelli, Ph.D., Department of Information Engineering, University of Padova, Via G. Gradenigo 6/B, 35131 Padova, Italy; email address cobelli@dei.unipd.it

could negatively influence the correct functioning of applications based on it. In particular, three issues of relevance can be pointed out:[24,25] (1) the presence of random noise makes CGM data uncertain;[26–28] (2) when comparing CGM with "gold standard" blood glucose (BG) references measured by laboratory instruments, delays (due to blood-to-interstitium glucose transport and sensor processing time[29]) and systematic underestimations/overestimations due to calibration problems are visible;[30–33] and (3) generating alerts some time before the CGM profile crosses hypoglycemic/hyperglycemic thresholds may help the mitigation of hypoglycemic/hyperglycemic critical events.[34]

In order to better illustrate these three issues, **Figure 1** shows a representative data set collected in a real type 1 diabetes mellitus (T1DM) patient consisting of a CGM time series (blue line) measured using the SEVEN Plus system (Dexcom Inc., San Diego, CA), and a time series of BG references (green dots, linearly interpolated to improve their inspection) measured simultaneously using the laboratory YSI 2300 apparatus (Yellow Springs Instruments, Yellow Spring, OH). In fact, the CGM time series displayed in the picture (1) is noisy—for example, note the portion of data circled in red in the time window 10:00–13:00; (2) lacks accuracy—note the delay in the time window 20:00–23:00 and the overestimation in the time interval 07:00–11:00; and (3) would allow generation of alerts only with some delay—compare the hypoglycemic threshold crossing of BG and CGM profiles around time 23:00.

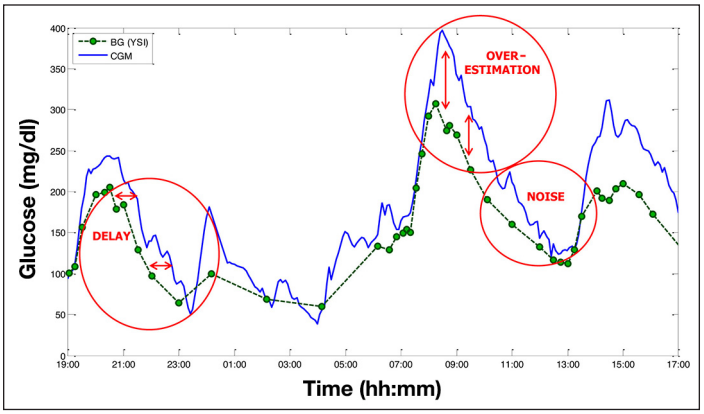

Figure 1. Representative T1DM subject, days 3–4: CGM (blue line) and BG references (green dots, linearly interpolated by dashed line). Issues related to uncertainty, accuracy and delay (see text) are evidenced by red circles.

We developed the "smart sensor" architecture concept that consists of a commercial CGM sensor and three software modules placed in cascade, each one specifically designed to face one of the three issues presented earlier. The aim of the smart sensor algorithms is to render CGM data more reliable and more accurate, and this can be of great benefit for several applications, e.g., hypoglycemic/hyperglycemic alert generation in an open-loop setting and AP implementations, in which uncertainty and accuracy of CGM data strongly influence the effectiveness of control action. In particular, in a clinically oriented paper,[35] we simulated the implementation of the smart CGM sensor concept by retrospectively applying algorithms developed by our research group[28,36,37] for denoising, signal enhancement, and prediction on a data set consisting of 24 real T1DM patients monitored simultaneously with a Dexcom SEVEN Plus sensor and a YSI. Results demonstrated that the smart CGM sensor outperforms the original CGM sensor in terms of precision, accuracy, and timeliness in the generation of alerts. This paper is intended to be a companion article to the article by Facchinetti and coauthors,[35] with the aim of illustrating the technical details of the algorithms and implementation issues to a more mathematically expert readership.

Architecture and Algorithms of the Smart Continuous Glucose Monitoring Sensor

The block scheme in **Figure 2** shows the architecture of the smart CGM sensor (box with green background). Conceptually, several software modules can be placed in cascade to a commercial CGM sensor (treated and represented as a black-box block), but here three modules (blocks represented with white background) are considered: (1) the denoising module contains an algorithm aimed at attenuating measurement noise, (2) the enhancement module embeds an algorithm that recalibrates CGM data to improve accuracy, and (3) the prediction module presents an algorithm for predicting in real time the future glucose concentration and possibly generating timelier alerts. Specific references for each of the blocks will be quoted later. The inputs of the ensemble of smart CGM sensor algorithms (arrows entering the modules) are: raw glucose concentration values supplied by the CGM sensor; some BG references (usually SMBG measurements, exploited by the enhancement module); and, if available (such optionality is represented by dashed instead of continuous input arrow), other information that could be relevant, such as times of meal, quantity, and composition, amount of insulin injected or delivered by the insulin pump, or quantification of physical

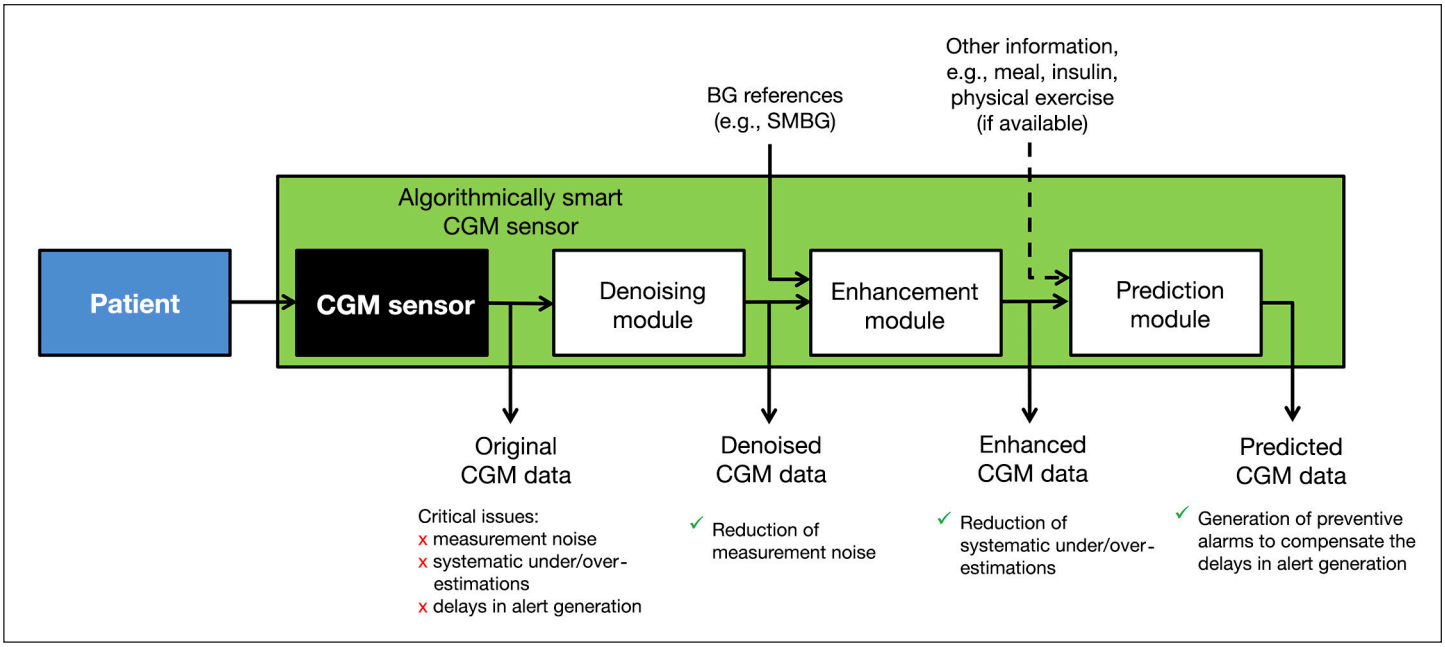

Figure 2. The smart CGM sensor architecture, consisting of a CGM sensor (black block) and three software modules for denoising, enhancement, and prediction applied in cascade. The denoising module receives in input CGM data and returns in output a filtered CGM profile. The enhancement module receives in input the denoised CGM data and (few) BG references, and returns in output enhanced (i.e., more accurate) CGM data. Finally, the prediction module receives in input denoised and enhanced CGM data (and possibly other additional inputs) and returns in output the forecast of future glucose value (for a given PH) on which "preventive" hypoglycemic/hyperglycemic alerts can be generated.

exercise (which could be exploited, in addition to past glucose history, by a certain class of prediction algorithms). The outputs (arrows exiting from the modules) are: denoised CGM data, which are more precise than original CGM data thanks to the attenuation of the measurement noise component; enhanced CGM data, which are more accurate with reduced under/overestimations; and future glucose levels forecasted for a preset prediction horizon (PH).

The Denoising Module

The denoising module is aimed to attenuate the random noise component that corrupts CGM data, i.e., to improve the precision of the glucose concentration values given in output by the CGM sensor. From a practical perspective, improving the smoothness of CGM data without introducing significant distortion (e.g., delays) is important to reduce the nuisance for the patient. In fact, the greater the variance of the random noise that corrupts the CGM data, the higher the probability that spurious crossings of hypoglycemic/hyperglycemic thresholds occur. In addition, a noisy CGM signal unavoidably deteriorates the effectiveness of closed-loop control in AP applications. To reduce measurement noise, real-time digital filtering is needed. The main problem to be faced is the presence of interindividual and intra-individual variability of signal-to-noise ratio on CGM data. To overcome possible suboptimality of approaches with fixed parameters, see referenced work;[24,25,27] for more detailed review aspects and a comparison of algorithms, the algorithm presented by Facchinetti and coauthors[28] is used. Briefly, this algorithm assumes that the CGM value measured at the discrete time k, i.e. $y(k)$, can be modeled as

$$y(k) = u(k) + v(k), \tag{1}$$

where $u(k)$ is the true (unknown) glycemic value and $v(k)$ is the random measurement noise, uncorrelated from $u(k)$ and with zero mean and (unknown) variance equal to $\sigma^2(k)$ (note the dependence of the noise variance on k). The denoising algorithm returns the estimate $\hat{u}(k)$ by exploiting *a priori* information formulated in a Bayesian setting. In particular, *a priori* knowledge on the smoothness of $u(t)$ is modeled as the double integration of white noise process

$$u(k) = 2u(k - 1) - u(k - 2) + w(k), \tag{2}$$

where $w(k)$ is assumed a zero mean white noise with (unknown) variance equal to $\lambda^2(k)$ (note the dependence of the signal variance on k). Every time a new glycemic reading $y(k)$ is produced by the CGM sensor, a window of N, with $N < k$, past CGM values is selected. Usually, N should be some tens, e.g., in the case of a 5 min sampling time, one can select a 3 h window, with $N = 36$ samples). Once N is selected, we can define the N-size vectors $\boldsymbol{y} = [y(k - N + 1)\ y(k - N + 2)\ ...\ y(k)]$, $\boldsymbol{u} = [u(k - N + 1)\ u(k - N + 2)\ ...\ u(k)]$, and $\boldsymbol{v} = [v(k - N + 1)\ v(k - N + 2)\ ...\ v(k)]$. Let us also consider the covariance matrix of $\boldsymbol{v}$ depending on the scale factor σ^2 (for simplicity, let us ignore, for a while, the dependence of σ^2 and λ^2 on k), i.e., $\Sigma_v = \sigma^2\boldsymbol{B}$, with $\boldsymbol{B}$-squared N-size positive definite matrix expressing our prior knowledge on the structure of the autocorrelation of $\boldsymbol{v}$. For instance, $\boldsymbol{B}$ is diagonal when noise samples are uncorrelated. If knowledge on noise autocorrelation is available, it can be easily incorporated in B, see referenced work for a denoising problem where the disturbance was modeled by an autoregressive process.[38] Then, according to results well established in the framework of Bayesian estimation theory,[39] the linear minimum variance estimator $\hat{u}$ is

$$\hat{\boldsymbol{u}} = (\boldsymbol{B}^{-1} + \gamma\boldsymbol{F}^T\boldsymbol{F})^{-1}\boldsymbol{B}^{-1}\boldsymbol{y}, \tag{3}$$

where $\boldsymbol{F}$ is an $n \times n$ matrix Toeplitz lower triangular matrix that, according to **Equation (2)**, has first column given by $[1, -2, 1\ 0\ \ldots\ 0]^T$, and $\gamma = \sigma^2/\lambda^2$ acts as a regularization parameter. A statistically based criterion is used in order to determine γ by fulfilling

$$\frac{\mathrm{WRSS}(\gamma)}{n - q(\gamma)} = \frac{\mathrm{WESS}(\gamma)}{q(\gamma)}, \tag{4}$$

where WRSS (quadratic sum of weighted residuals) = $(\boldsymbol{y} - \hat{\boldsymbol{u}})^T\boldsymbol{B}^{-1}(\boldsymbol{y} - \hat{\boldsymbol{u}})$, WESS (quadratic sum of weighed estimates) = $\hat{\boldsymbol{u}}^T\boldsymbol{F}^T\boldsymbol{F}\hat{\boldsymbol{u}}$, and $q(\gamma)$ (equivalent degrees of freedom) = $\mathrm{trace}(\boldsymbol{B}^{1/2}(\boldsymbol{B}^{-1}+\gamma\boldsymbol{F}^T\boldsymbol{F})^{-1}\boldsymbol{B}^{-1/2})$, see referenced work for proof and details.[40,41] Then an estimate of the noise variance σ^2 can be derived as

$$\sigma^2 = \frac{\mathrm{WRSS}(\gamma)}{n - q(\gamma)}. \tag{5}$$

In practice, every time a new glucose reading is produced by the CGM sensor, γ can be computed on the current time frame in order to deal with the dependency of σ^2 and λ^2 on k.

The algorithm has several remarkable features, e.g.,

i. it is self-tunable, meaning that all unknown filter parameters $\sigma^2(k)$ and $\lambda^2(k)$ are automatically estimated without the need of user intervention;

ii. it is adaptive, i.e., the values of $\sigma^2(k)$ and $\lambda^2(k)$ used in the filtering procedure are re-estimated at any k, allowing the denoising module to cope with the interindividual and the intraindividual variability of the signal-to-noise ratio;

iii. the Bayesian embedding allows calculating the covariance matrix of the estimation error $\tilde{\boldsymbol{u}} = \boldsymbol{u} - \hat{\boldsymbol{u}}$, whose square root diagonal elements represent an estimation of the confidence interval of the denoised CGM values, which can be used, e.g., for alert generation or in fault detection;[42]

iv. the estimate of σ^2 obtained by **Equation (5)** gives the power of the measurement noise of the sensor, and an analysis of its variability with k could help in detecting portion of unreliable CGM data; and

v. the structure of $\boldsymbol{B}$ can be chosen in order to reflect expectations/knowledge on noise autocorrelation, e.g., white rather than colored.

The Enhancement Module

The enhancement module is aimed to improve CGM accuracy. To do this, it is key to take into account that differences between reference BG measurements and CGM data as those visible in **Figure 1** can be due not only to plasma-

to-interstitial fluid glucose kinetics, but also to suboptimal calibrations and time-variance in sensor behavior. Many examples of proposed enhancement/calibration algorithms are available.[30–33,43] In the smart sensor concept,[35] the algorithm exploited in the enhancement module is the one proposed and assessed in Guerra and coauthors.[36] Briefly, the method consists in four main steps.

(A) In the first step, we fill a vector, $\boldsymbol{x}$, with $m \geq 2$ SMBG measurements, i.e., $\boldsymbol{x} = \{\text{SMBG}(T_i)\}$, $I = 1, 2, \ldots, m$, and another vector, $\boldsymbol{y}$, with n CGM samples, i.e., $\boldsymbol{y} = \{\text{CGM}(t_j)\}$, $j = 1, 2, \ldots, n$, collected in the same temporal window containing the SMBG values, i.e., $T_1 \geq t_1$ and $T_m \leq t_n$. Preferably, the window should include the glucose rising front after a meal to reduce the impact of possible SMBG measurement error on the calculation of the parameters of the linear regressor in step (C).[44] The integers n and m can be viewed as user parameters.

(B) In the second step, we first assume that, at continuous time t, each CGM reading can be modeled as:

$$y(t_j) = \int_{-\infty}^{t_j} g(t_j,\omega)\text{BG}(\omega) + v(t_j), \tag{6}$$

where $g(t,\omega)$ is the impulse response of the BG-to-interstitial-glucose system, i.e., the hypothetical time course of interstitial glucose produced by a Dirac pulse BG centered at time t_j, and $v(t_j)$ is zero-mean additive measurement noise with (unknown) variance already considered in **Equations** (**1**) and (**3**). While **Equation** (**6**) allows the plug-in of a generic structure for $g(t,\omega)$, in Guerra and coauthors,[36] we exploited a time-invariant single exponential impulse response derived from the two-compartment model of BG-to-interstitial-glucose kinetics developed by Rebrin and coauthors,[45] i.e., the response to a Dirac pulse centered at time 0 is

$$g(t) = \frac{1}{\tau} e^{-\frac{t}{\tau}}, \tag{7}$$

where τ is the time constant of the model. Then, from Equation (6), we provide estimates of BG on the same grid of the CGM signal, i.e., $\widehat{\mathbf{BG}} = \{\widehat{\text{BG}}(t_j)\}$, $j = 1,2,\ldots,n$ by a stochastic formulation of the Phillips–Tikhonov deconvolution method,[40] which ultimately leads us to compute

$$\widehat{\mathbf{BG}} = (\boldsymbol{G}^T\boldsymbol{\Sigma}_v^{-1}\boldsymbol{G} + \gamma\boldsymbol{F}^T\boldsymbol{F})^{-1}\boldsymbol{\Sigma}_v^{-1}\boldsymbol{G}\boldsymbol{y}, \tag{8}$$

where $\boldsymbol{\Sigma}_v = \sigma^2\boldsymbol{B}$ is the $n \times n$ covariance matrix expressing our prior knowledge on the structure of the autocorrelation of $n \times 1$ vector $\boldsymbol{v}$ (possible structures of $\boldsymbol{B}$ were discussed in earlier), $\boldsymbol{G}$ is a lower triangular $n \times n$ Toeplitz matrix (having as first column the definite integrals of $g(t)$ of **Equation** (**7**) on the CGM sampling grid), while $\boldsymbol{F}$ and γ have the same meaning as in **Equation** (**3**). The optimal value of γ is determined using the same criterion of **Equation** (**4**). Note that $\widehat{\mathbf{BG}}$ should correspond to the BG profile related to the selected portion of CGM data in case of optimal calibration, i.e., in absence of any error.

(C) In the third step, least squares linear regression is used to fit the $\boldsymbol{m}$ SMBG samples contained in $\boldsymbol{x} = \{\text{SMBG}(T_i)\}$ against the m-size vector $\boldsymbol{\psi}$ containing those elements that are relative to T_i ($I = 1, \ldots m$):

$$\boldsymbol{x} = a\,\boldsymbol{\psi} + b. \tag{9}$$

In an optimal scenario, we should expect $(a,b) = (1,0)$. In general, but in particular when the CGM sensor is not optimally calibrated, a and b take values different from (1,0).

(D) The estimated regression parameters (a,b) of **Equation** (**9**) are finally used to "enhance" CGM data that will be collected at time $t_k \geq t_n$, as

$$\text{CGM}_{\text{enhanced}}(t_k) = a\ \text{CGM}(t_k) + b. \tag{10}$$

As discussed in detail by Guerra and coauthors,[36] this enhancement algorithm has some advantages over other literature approaches:

i. it explicitly takes into account the influence of blood-to-interstitium glucose transport and possible delays due to sensor technology and denoising step before applying regression, with the advantage that the time constant τ of the model can be individualized to the specific patient;

ii. all the parameters of this enhancement algorithm can be automatically determined in real time, while other literature procedures require an offline tuning (e.g., in the extended Kalman filter previously proposed,[30,31] the unknown covariance matrices cannot be estimated in real time);

iii. similarly to the denoising algorithm, the structure chosen for Σ_v can be chosen according to available knowledge on measurement noise autocorrelation.

The Prediction Module

Several prediction strategies have been proposed in the literature (see referenced work for details on the methodologies used[37,46–51] and their application), combined with an alert generation system to prevent hypoglycemic events, performed in an *in silico* environment,[9,10] and with preliminary application in clinical research centers.[11–13] The architecture depicted in **Figure 2** allows the exploitation of meal, insulin, and physical activity information, and sophisticated methods can be plugged in the prediction module block. Given that such information was not available in the data set studied, in previous work,[35] we implemented the simple algorithm presented by Sparacino and coauthors[37] and based an autoregressive model of the first order, AR(1), corresponding to the following difference equation:

$$y(k) = \alpha\, y(k-1) + \eta(k), \tag{11}$$

where $y(k)$ is the CGM value at discrete time k, α is the parameter of the model, and $\eta(k)$ is a random white noise process, with zero mean and variance ρ^2. The estimation of the parameters vector (α, ρ^2) is performed in real time using a recursive least square strategy. All the past CGM data participate with different relative weights to the estimation of the parameters vector. The weighting strategy is based on a parameter μ, named forgetting factor, which can vary in the interval [0,1]. In the estimation procedure, the sample collected q time steps before, i.e., $y(k - q)$, is assigned the weight μ^q. The model is then used to predict the glucose level T steps ahead $\hat{y}(k + T)$, iterating the model equation for $j = k + 1, k + 2, \ldots, k + T$, with $\eta = 0$, i.e.,

$$\hat{y}(k + T|k) = \alpha^T\, y(k). \tag{12}$$

The value of μ has been fixed for all patients and determined by minimizing the performance index J.[52] Specifically, for the Dexcom SEVEN Plus data set, the minimization of the index J returned an optimal $\mu = 0.925$. Then, from a practical perspective, the predicted value at time t, $\hat{y}(k + T|k)$ and the predicted value at time $t - 1$, $\hat{y}(k - 1 + T|k - 1)$, are taken into account and compared with hypoglycemic and hyperglycemic thresholds. If $\hat{y}(k - 1 + T|k - 1) \geq 70$ mg/dl and $\hat{y}(k + T|k) < 70$ mg/dl, a hypoglycemic threshold crossing is predicted, thus a preventive hypo-alert at time k is generated. Similarly, if $\hat{y}(k - 1 + T|k - 1) \leq 180$ mg/dl and $\hat{y}(k + T|k) > 180$ mg/dl, a hyperglycemic threshold crossing is predicted, thus a preventive hyper-alert at time t is generated.

The principal features of the selected prediction algorithm are that

i. it is self-tunable and adaptive, i.e., the parameter vector (α, ρ^2) is estimated in real time every time a new CGM value is available, allowing it to adapt to variations in glucose dynamics and

ii. a recursive algorithm implementation allows us to maintain very low memory and processing requirements.

Evaluation of the Smart Continuous Glucose Monitoring Sensor on Real Data

In the companion clinical article,[35] the smart CGM sensor concept was retrospectively tested on data collected in 24 T1DM patients within the AP@home FP7-EU project.[53] Each data set consists of a 7-day profile of CGM data measured

using the SEVEN Plus sensor and 1-day high-frequency BG measurements (YSI 2300) collected in parallel to CGM during day 3 (which was spent by the patient in a clinical research center). The companion article[35] provides the details of the protocol,[35] a comprehensive discussion of the results and clinical interpretation, and the potential impact on diabetes treatment. Here, we will focus only on some representative examples that allow some technical considerations in terms of metrics usable for performance assessment.

Figure 3 illustrates a graphical example of results obtained by the denoising module on data of subject 3. The original CGM time series (blue line) is compared with the denoised CGM profile (red line). To improve the readability, a zoom of day 2 is displayed. The improvement in the smoothness of CGM and consequent reduction of spurious oscillations is clearly evident, e.g., in both time intervals 02:00–04:00 and 21:00–23:00. To quantify the improvement, we resort to the energy of second-order differences (ESOD). In fact, as well established in the context of Phillips–Tikhonov regularization,[54] the regularity of a time series $z = \{z(1),z(2),\ldots,z(N)\}$ of length N, with samples collected in a uniform grid, can be measured by

$$\mathrm{ESOD}(z) = \sum_{i=3}^{N}(z(i) - 2(z - 1) + z(i - 2))^2. \quad (13)$$

The larger the ESOD, the less smooth the time series (see referenced work for use in CGM applications[27,28,37,52]). In this particular example, the ESOD value is reduced from 3.8 to 1.9, confirming the evident improvement. The boxplot of **Figure 4A** shows that, considering all 24 subjects, ESOD reduction is significant, with a median ESOD value lowered more than 50% (from 1.4 to 0.6; $p = .001$).

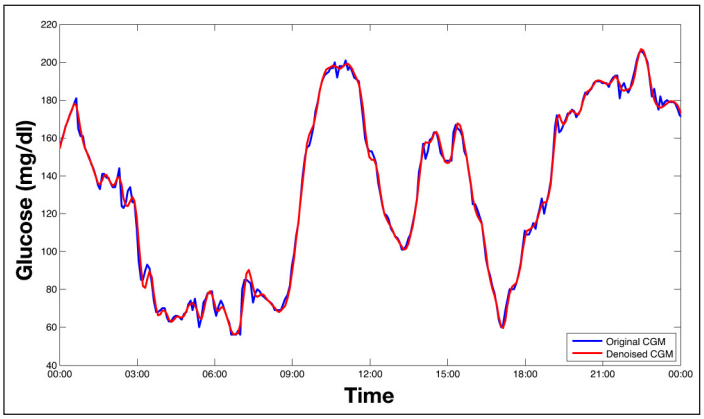

Figure 3. Results of the application of denoising module on subject 3, day 2. Data of day 2 are plotted to improve visualization. Original (blue) and denoised (red) CGM data are shown.

With regard to the enhancement step, **Figure 5** depicts the original CGM profile (blue), the enhanced CGM time series (red), and BG reference data (green dots) in subject 12. We focused on the time interval from 18:00 of day 3 to 16:00 of day 4, being the time window in which BG references are available. The improvement in the accuracy of the sensor is evidently displayed in the reduction of the overestimation in the time interval 10:00–16:00. Of potential clinical importance is the reduction of the underestimation around 01:00. In fact, assuming that the unrealistic negative swing around 01:00 in CGM is spurious, the original CGM time series would have "potentially" triggered a false hypoglycemic alert around 01:00 and needlessly woken up the patient. Thanks to the enhancement module, this false alert would have been avoided. The improvement of accuracy in subject 12 is confirmed by quantitative indexes, e.g., by a reduction of mean absolute relative difference (MARD) index[55] from 30.6% to 6.8%. The boxplot of **Figure 4B** summarizes the results on the whole database. The median MARD value is significantly reduced from 13.1% to 9.6% ($p = .003$), evidence that the smart CGM sensor (SEVEN Plus and algorithms for denoising and enhancement, the last one exploiting the same number of SMBG measurements used for calibration) outperforms the basic CGM sensor (SEVEN Plus). Of note also is that, as evidenced in the clinically oriented article,[35] the MARD value achieved by the algorithmically smart CGM sensor (9.6%) is lower than that of another CGM device, the Enlite sensor (Medtronic Diabetes, Northridge, CA), whose MARD value was estimated at approximately 13.8%.[56] Similar conclusions could be drawn by considering other popular metrics besides MARD, such as the Clarke error grid,[57] the continuous glucose error grid analysis,[58] relative difference,[23] or MARD per BG.[23]

Figure 6 shows an example of the prediction of future glucose concentration, performed with PH = 30 min, given in output by the prediction module for subject 5. Data are shown for CGM (blue line) and predicted CGM (red line). To improve the readability of the picture, a zoom of the time interval 07:00–15:00 of day 4 has been selected. One hypoglycemic alert is generated on the basis of CGM data at time 12:35 (blue arrow). The prediction module

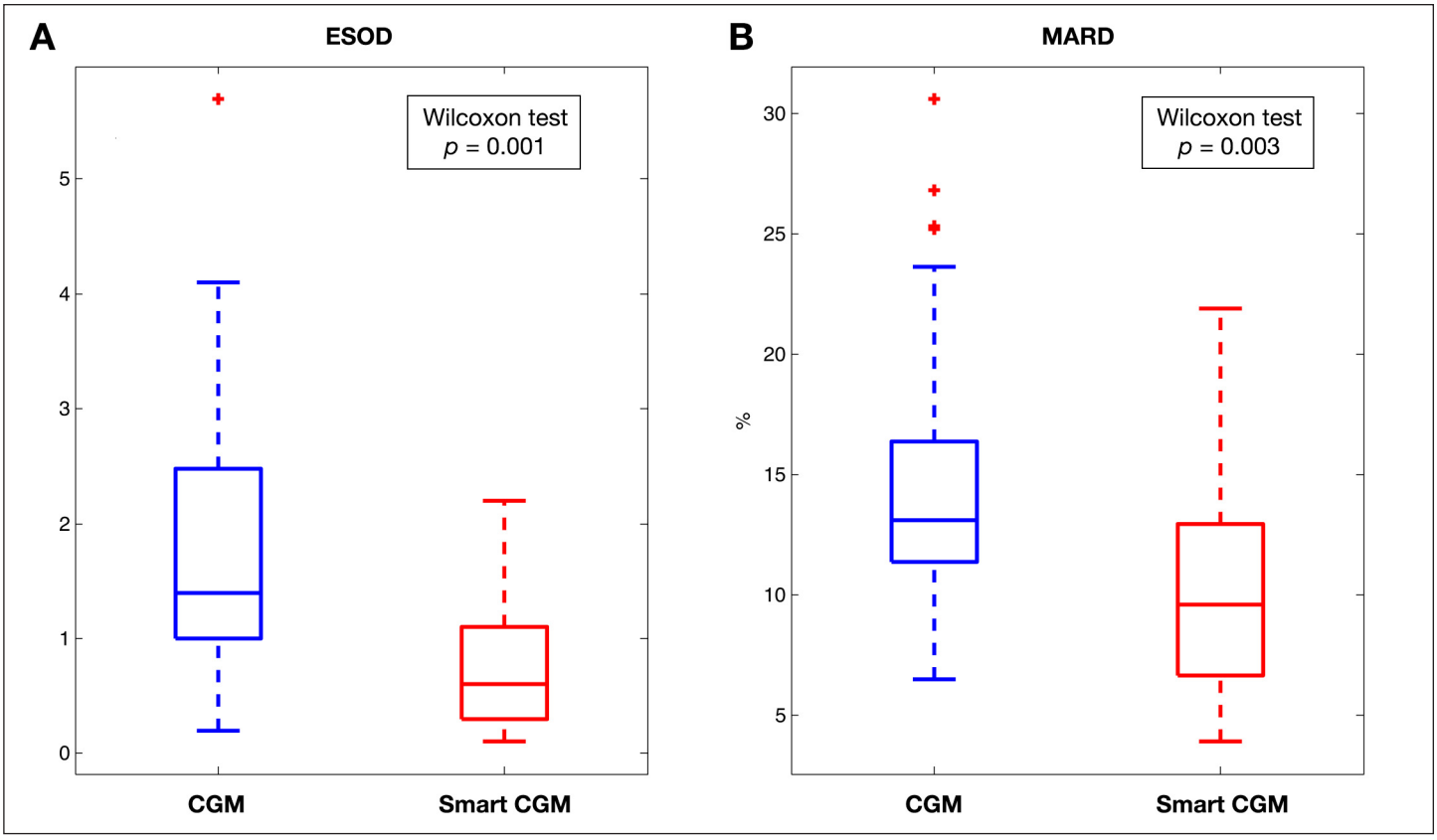

Figure 4. Boxplots of selected comparison indexes. Blue and red refers to CGM and smart CGM configurations, respectively. The result of the application of Wilcoxon test is reported. **(A)** The ESOD of glucose profile. **(B)** The MARD of CGM data versus BG references.

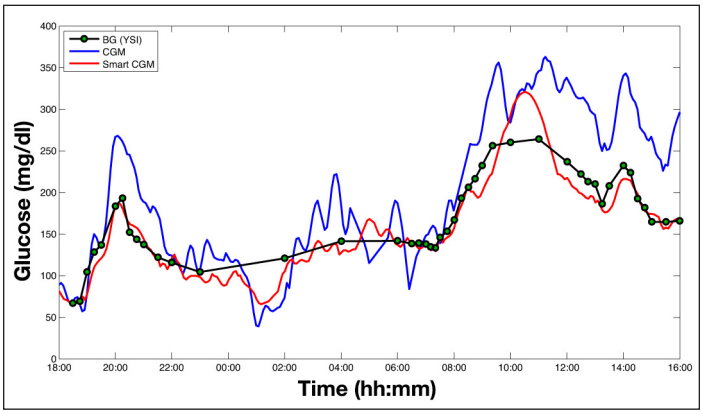

Figure 5. Results of the application of enhancement module on subject 12, days 3–4. Original (blue) and enhanced (red) CGM data and BG references (green dots) are shown.

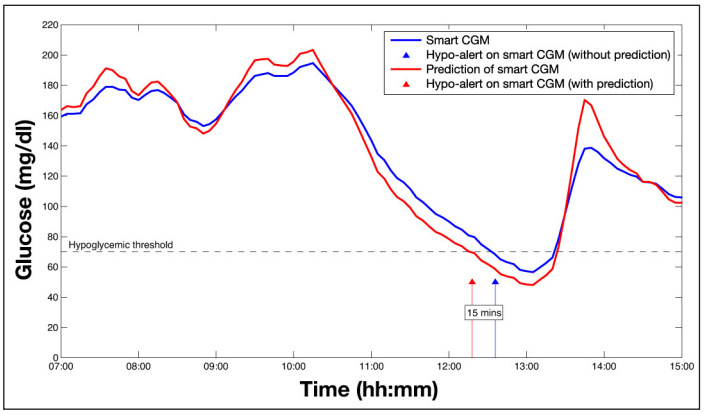

Figure 6. Results of the application of prediction module on subject 5, day 4. Smart CGM data (blue) and real-time prediction (red) obtained with PH of 30 min. Vertical arrows (same color codes) indicate the alerts that could be generated at the crossing the hypoglycemic threshold. In this case, a temporal gain of 15 min in facing the event could be obtained thanks to prediction.

allows generating a preventive hypoglycemic alert at time 12:20 (red arrow), meaning that the critical event can be predicted 15 min before the happening (with the possibility of acting timely to avoid, or at least mitigate, the event). In the whole database, a total of 60 hypoglycemic episodes were detected by CGM data. All hypo-events were detected correctly by the prediction algorithm. Specifically, the prediction algorithm was able to forecast 55 hypo-events (91.6%) within the chosen PH with a positive anticipation (i.e., >0 min), meaning that almost all events were predicted before their occurrence (i.e., before the alert was triggered by the CGM profile). Numerically, the amount of time gained before the hypoglycemic threshold crossing of the smart CGM trace is 15.1 min (median value). In the

evaluation of the performance of hypoglycemic/hyperglycemic alert generation system, it is important to quantify also the percentage of false alerts generated on the basis of the prediction. In this case, we assume that an alert generated by the prediction is a false positive if the CGM trace does not fall below the hypoglycemic threshold (70 mg/dl) in the following 60 min. The number of false positives generated by the algorithm is 19, which corresponds to the 25.7% of the total amounts of alerts. Note that the paradigm we chose for the evaluation of the alerts is simple and has the limitation of treating all false negatives equally, independent of the seriousness of the event (e.g., the minimum glucose concentration value reached in correspondence to the false alert).

Conclusions

Continuous glucose monitoring sensors are key in several applications, for instance, in systems for real-time generation of hypoglycemic and closed-loop algorithms for the AP. However, CGM sensor performance is still suboptimal in terms of accuracy and precision, and some margins of improvement are present at the algorithm level. We presented the "smart sensor" concept, i.e., the idea of rendering "smart" a commercial CGM sensor by placing suitable software modules in cascade to it. The idea was quantitatively assessed on data of 24 patients by Facchinetti and coauthors,[35] demonstrating that smoothness of CGM profile (measured by ESOD) can be improved 1accuracy (measured by MARD against YSI references) by approximately 27%, and anticipated hypo-events alert generation by approximately 15 min (with a number of false alerts of 25.7%). However, in the work of Facchinetti and coauthors,[35] given the clinically oriented readership, there was no room for technical details, and the reproducibility of our results in other laboratories could thus be difficult. This articles is considered as a companion of the previous article,[35] with the aim of illustrating the technical details of the algorithms, paying attention to implementation aspects, in order to render them fully and easily reproducible.

While the architecture of the smart sensor concept of **Figure 2** is general, the algorithms specifically considered in this article have some important features in common. The first is real-time functioning. The second is adaptability, because they work in cascade to any CGM sensor, independently from the manufacturer. The third is their independency, i.e., if one module is removed, the others still work. The modules are placed in the order displayed in **Figure 2** to maximize the global output. In fact, before performing any enhancement to increase accuracy, it is essential to remove the measurement noise from CGM data to limit the propagation of measurement error. Similarly, the prediction is even more efficient and reliable if CGM data are both smoother and enhanced.

We can conclude that suitable real-time algorithms can render CGM sensor more reliable with possible great benefit in applications based on CGM devices, e.g., AP prototypes in which precision and accuracy of CGM data strongly influence the control action. Further margins of improvement of the algorithms can be pursued in the coming years. For instance, given the common framework of the denoising and the enhancement approaches, the two algorithms can be merged and performed in the same step to reduce the complexity. Another possible improvement concerns the prediction module, specifically the inclusion of additional information in the prediction algorithm (see dashed input arrow in the prediction module block of **Figure 2**), such as meals (see for example referenced work for a method exploiting neural networks[49]) or physical activity, which are not exploited by the current prediction algorithm.

Funding:

This study was supported by the EU project AP@home, an integrating large-scale project of the 7th Framework Programme (2010–2014), grant 247138.

Acknowledgments:

Data were collected, under the aegis of FP7 EU project "AP@home," at Academic Medical Center Amsterdam (Amsterdam, The Netherlands), Medical University of Graz (Graz, Austria), Profil Institute for Metabolic Research GmbH (Neuss, Germany), and Department of Clinical and Experimental Medicine, University of Padova (Padova, Italy).

References:

1. Klonoff DC. Continuous glucose monitoring: Roadmap for 21st century diabetes therapy. Diabetes Care. 2005;28(5):1231–9.
2. McGarraugh G. The chemistry of commercial continuous glucose monitors. Diabetes Technol Ther. 2009;11 Suppl 1:S17–24.
3. Cox M. An overview of continuous glucose monitoring systems. J Pediatr Health Care. 2009;23(5):344–7.

4. Joubert M, Reznik Y. Personal continuous glucose monitoring (CGM) in diabetes management: review of the literature and implementation for practical use. Diabetes Res Clin Pract. 2012;96(3):294–305.
5. Sparacino G, Zanon M, Facchinetti A, Zecchin C, Maran A, Cobelli C. Italian contributions to the development of continuous glucose monitoring sensors for diabetes management. Sensors (Basel). 2012;12(10):13753–80.
6. Juvenile Diabetes Research Foundation Continuous Glucose Monitoring Study Group, Tamborlane WV, Beck RW, Bode BW, Buckingham B, Chase HP, Clemons R, Fiallo-Scharer R, Fox LA, Gilliam LK, Hirsch IB, Huang ES, Kollman C, Kowalski AJ, Laffel L, Lawrence JM, Lee J, Mauras N, O'Grady M, Ruedy KJ, Tansey M, Tsalikian E, Weinzimer S, Wilson DM, Wolpert H, Wysocki T, Xing D. Continuous glucose monitoring and intensive treatment of type 1 diabetes. N Engl J Med. 2008;359(14):1464–76.
7. Rodbard D. Glycemic variability: measurement and utility in clinical medicine and research--one viewpoint. Diabetes Technol Ther. 2011;13(11):1077–80.
8. McGarraugh G, Bergenstal R. Detection of hypoglycemia with continuous interstitial and traditional blood glucose monitoring using the FreeStyle Navigator Continuous Glucose Monitoring System. Diabetes Technol Ther. 2009;11(3):145–50.
9. Zecchin C, Facchinetti A, Sparacino G, Cobelli C. Reduction of number and duration of hypoglycemic events by glucose prediction methods: a proof-of-concept in silico study. Diabetes Technol Ther. 2013;15(1):66–77.
10. Hughes CS, Patek SD, Breton MD, Kovatchev BP. Hypoglycemia prevention via pump attenuation and red-yellow-green "traffic" lights using continuous glucose monitoring and insulin pump data. J Diabetes Sci Technol. 2010;4(5):1146–55.
11. Cameron F, Wilson DM, Buckingham BA, Arzumanyan H, Clinton P, Chase HP, Lum J, Maahs DM, Calhoun PM, Bequette BW. Inpatient studies of a Kalman-filter-based predictive pump shutoff algorithm. J Diabetes Sci Technol. 2012;6(5):1142–7.
12. Dassau E, Cameron F, Lee H, Bequette BW, Zisser H, Jovanovic L, Chase HP, Wilson DM, Buckingham BA, Doyle FJ 3rd. Real-Time hypoglycemia prediction suite using continuous glucose monitoring: a safety net for the artificial pancreas. Diabetes Care. 2010;33(6):1249–54.
13. Buckingham B, Chase HP, Dassau E, Cobry E, Clinton P, Gage V, Caswell K, Wilkinson J, Cameron F, Lee H, Bequette BW, Doyle FJ 3rd. Prevention of nocturnal hypoglycemia using predictive alarm algorithms and insulin pump suspension. Diabetes Care. 2010;33(5):1013–7.
14. Weinzimer SA, Steil GM, Swan KL, Dziura J, Kurtz N, Tamborlane WV. Fully automated closed-loop insulin delivery versus semiautomated hybrid control in pediatric patients with type 1 diabetes using an artificial pancreas. Diabetes Care. 2008;31(5):934–9.
15. Hovorka R, Allen JM, Elleri D, Chassin LJ, Harris J, Xing D, Kollman C, Hovorka T, Larsen AM, Nodale M, De Palma A, Wilinska ME, Acerini CL, Dunger DB. Manual closed-loop insulin delivery in children and adolescents with type 1 diabetes: a phase 2 randomised crossover trial. Lancet. 2010;375(9716):743–51.
16. Kovatchev B, Cobelli C, Renard E, Anderson S, Breton M, Patek S, Clarke W, Bruttomesso D, Maran A, Costa S, Avogaro A, Dalla Man C, Facchinetti A, Magni L, De Nicolao G, Place J, Farret A. Multinational study of subcutaneous model-predictive closed-loop control in type 1 diabetes mellitus: summary of the results. J Diabetes Sci Technol. 2010;4(6):1374–81.
17. Breton M, Farret A, Bruttomesso D, Anderson S, Magni L, Patek S, Dalla Man C, Place J, Demartini S, Del Favero S, Toffanin C, Hughes-Karvetski C, Dassau E, Zisser H, Doyle FJ 3rd, De Nicolao G, Avogaro A, Cobelli C, Renard E, Kovatchev B; International Artificial Pancreas Study Group. Fully integrated artificial pancreas in type 1 diabetes: modular closed-loop glucose control maintains near normoglycemia. Diabetes. 2012;61(9):2230–7.
18. Cobelli C, Renard E, Kovatchev BP, Keith-Hynes P, Ben Brahim N, Place J, Del Favero S, Breton M, Farret A, Bruttomesso D, Dassau E, Zisser H, Doyle FJ 3rd, Patek SD, Avogaro A. Pilot studies of wearable outpatient artificial pancreas in type 1 diabetes. Diabetes Care. 2012;35(9):e65–7.
19. Russell SJ, El-Khatib FH, Nathan DM, Magyar KL, Jiang J, Damiano ER. Blood glucose control in type 1 diabetes with a bihormonal bionic endocrine pancreas. Diabetes Care. 2012;35(11):2148–55.
20. Phillip M, Battelino T, Atlas E, Kordonouri O, Bratina N, Miller S, Biester T, Stefanija MA, Muller I, Nimri R, Danne T. Nocturnal glucose control with an artificial pancreas at a diabetes camp. N Engl J Med. 2013;368(9):824–33.
21. McGarraugh GV, Clarke WL, Kovatchev BP. Comparison of the clinical information provided by the FreeStyle Navigator continuous interstitial glucose monitor versus traditional blood glucose readings. Diabetes Technol Ther. 2010;12(5):365–71
22. Langendam M, Luijf YM, Hooft L, Devries JH, Mudde AH, Scholten RJ. Continuous glucose monitoring systems for type 1 diabetes mellitus. Cochrane Database Syst Rev. 2012;1:CD008101.
23. Damiano ER, El-Khatib FH, Zheng H, Nathan DM, Russell SJ. A comparative effectiveness analysis of three continuous glucose monitors. Diabetes Care. 2013;36(2):251–9.
24. Sparacino G, Facchinetti A, Cobelli C. "Smart" continuous glucose monitoring sensors: on-line signal processing issues. Sensors (Basel). 2010;10(7):6751–72.
25. Bequette BW. Continuous glucose monitoring: real-time algorithms for calibration, filtering, and alarms. J Diabetes Sci Technol. 2010;4(2):404–18.
26. Palerm CC, Willis JP, Desemone J, Bequette BW. Hypoglycemia prediction and detection using optimal estimation. Diabetes Technol Ther. 2005;7(1):3–14.
27. Facchinetti A, Sparacino G, Cobelli C. An online self-tunable method to denoise CGM sensor data. IEEE Trans Biomed Eng. 2010;57(3):634–41.
28. Facchinetti A, Sparacino G, Cobelli C. Online denoising method to handle intraindividual variability of signal-to-noise ratio in continuous glucose monitoring. IEEE Trans Biomed Eng. 2011;58(9):2664–71.
29. Aussedat B, Dupire-Angel M, Gifford R, Klein JC, Wilson GS, Reach G. Interstitial glucose concentration and glycemia: implications for continuous subcutaneous glucose monitoring. Am J Physiol Endocrinol Metab. 2000;278(4):E716–28.
30. Knobbe EJ, Buckingham B. The extended Kalman filter for continuous glucose monitoring. Diabetes Technol Ther. 2005;7(1):15–27.

31. Facchinetti A, Sparacino G, Cobelli C. Enhanced accuracy of continuous glucose monitoring by online extended kalman filtering. Diabetes Technol Ther. 2010;12(5):353–63.

32. Rossetti P, Bondia J, Vehí J, Fanelli CG. Estimating plasma glucose from interstitial glucose: the issue of calibration algorithms in commercial continuous glucose monitoring devices. Sensors (Basel). 2010;10(12):10936–52.

33. Barceló-Rico F, Bondia J, Díez JL, Rossetti P. A multiple local models approach to accuracy improvement in continuous glucose monitoring. Diabetes Technol Ther. 2012;14(1):74–82

34. Kamath A, Mahalingam A, Brauker J. Methods of evaluating the utility of continuous glucose monitor alerts. J Diabetes Sci Technol. 2010;4(1):57–66.

35. Facchinetti A, Sparacino G, Guerra S, Luijf YM, DeVries JH, Mader JK, Ellmerer M, Benesch C, Heinemann L, Bruttomesso D, Avogaro A, Cobelli C; AP@home Consortium. Real-time improvement of continuous glucose monitoring accuracy: the smart sensor concept. Diabetes Care. 2013;36(4):793–800.

36. Guerra S, Facchinetti A, Sparacino G, Nicolao GD, Cobelli C. Enhancing the accuracy of subcutaneous glucose sensors: a real-time deconvolution-based approach. IEEE Trans Biomed Eng. 2012;59(6):1658–69.

37. Sparacino G, Zanderigo F, Corazza S, Maran A, Facchinetti A, Cobelli C. Glucose concentration can be predicted ahead in time from continuous glucose monitoring sensor time-series. IEEE Trans Biomed Eng. 2007;54(5):931–7.

38. D'Avanzo C, Schiff S, Amodio P, Sparacino G. A Bayesian method to estimate single-trial event-related potentials with application to the study of the P300 variability. J Neurosci Methods. 2011;198(1):114–24.

39. Anderson BD, Moore JB. Optimal filtering. Mineola: Dover Publications; 2005.

40. De Nicolao G, Sparacino G, Cobelli C. Nonparametric input estimation in physiological systems: problems, methods and case studies. Automatica. 1997;33(5):851–70.

41. Sparacino G, Cobelli C. A stochastic deconvolution method to reconstruct insulin secretion rate after a glucose stimulus. IEEE Trans Biomed Eng. 1996;43(5):512–29.

42. Facchinetti A, Del Favero S, Sparacino G, Cobelli C. An online failure detection method of the glucose sensor-insulin pump system: improved overnight safety of type-1 diabetic subjects. IEEE Trans Biomed Eng. 2013;60(2):406–16.

43. Kuure-Kinsey M, Palerm CC, Bequette BW. A dual-rate Kalman filter for continuous glucose monitoring. Conf Proc IEEE Eng Med Biol Soc. 2006;1:63–6.

44. King C, Anderson SM, Breton M, Clarke WL, Kovatchev BP. Modeling of calibration effectiveness and blood-to-interstitial glucose dynamics as potential confounders of the accuracy of continuous glucose sensors during hyperinsulinemic clamp. J Diabetes Sci Technol. 2007;1(3):317–22.

45. Rebrin K, Steil GM, van Antwerp WP, Mastrototaro JJ. Subcutaneous glucose predicts plasma glucose independent of insulin: implications for continuous monitoring. Am J Physiol. 1999;277(3 Pt 1):E561–71.

46. Gani A, Gribok AV, Rajaraman S, Ward WK, Reifman J. Predicting subcutaneous glucose concentration in humans: data-driven glucose modeling. IEEE Trans Biomed Eng. 2009;56(2):246–54.

47. Pérez-Gandía C, Facchinetti A, Sparacino G, Cobelli C, Gómez EJ, Rigla M, de Leiva A, Hernando ME. Artificial neural network algorithm for online glucose prediction from continuous glucose monitoring. Diabetes Technol Ther. 2010;12(1):81–8.

48. Pappada SM, Cameron BD, Rosman PM, Bourey RE, Papadimos TJ, Olorunto W, Borst MJ. Neural network-based real-time prediction of glucose in patients with insulin-dependent diabetes. Diabetes Technol Ther. 2011;13(2):135–41.

49. Zecchin C, Facchinetti A, Sparacino G, De Nicolao G, Cobelli C. Neural network incorporating meal information improves accuracy of short-time prediction of glucose concentration. IEEE Trans Biomed Eng. 2012;59(6):1550–60.

50. Naumova V, Pereverzyev SV, Sivananthan S. A meta-learning approach to the regularized learning-case study: blood glucose prediction. Neural Netw. 2012;33:181–93.

51. Eren-Oruklu M, Cinar A, Rollins DK, Quinn L. Adaptive system identification for estimating future glucose concentrations and hypoglycemia alarms. Automatica (Oxf). 2012;48(8):1892–7.

52. Facchinetti A, Sparacino G, Trifoglio E, Cobelli C. A new index to optimally design and compare continuous glucose monitoring glucose prediction algorithms. Diabetes Technol Ther. 2011;13(2):111–9.

53. AP@home, EU-FP7 project website. http://www.apathome.eu/. Accessed March 8, 2013.

54. Tikhonov AN, Arsenin VY. Solutions of ill-posed problems. Washington DC: Winston; 1977.

55. Kovatchev B, Anderson S, Heinemann L, Clarke W. Comparison of the numerical and clinical accuracy of four continuous glucose monitors. Diabetes Care. 2008;31(6):1160–4.

56. Keenan DB, Mastrototaro JJ, Zisser H, Cooper KA, Raghavendhar G, Lee SW, Yusi J, Bailey TS, Brazg RL, Shah RV. Accuracy of the Enlite 6-day glucose sensor with guardian and Veo calibration algorithms. Diabetes Technol Ther. 2012;14(3):225–31.

57. Clarke W, Kovatchev B. Statistical tools to analyze continuous glucose monitor data. Diabetes Technol Ther. 2009;11 Suppl 1:S45–54.

58. Kovatchev BP, Gonder-Frederick LA, Cox DJ, Clarke WL. Evaluating the accuracy of continuous glucose-monitoring sensors: continuous glucose-error grid analysis illustrated by TheraSense Freestyle Navigator data. Diabetes Care. 2004;27(8):1922–8.